Journal of Coordination Chemistry

ISSN: 0095-8972 (Print) 1029-0389 (Online) Journal homepage: http://www.tandfonline.com/loi/gcoo20

A 2-D dysprosium-organic complex constructed from 6,7-dihydropyrido(2,3-d)pyridazine-5,8-dione and oxalic acid: synthesis, characterization and photoluminescence

Yunshan Zhou, Junmei Sun, Waqar Ahmad, Lijuan Zhang & Zonghai Shi

To cite this article: Yunshan Zhou, Junmei Sun, Waqar Ahmad, Lijuan Zhang & Zonghai Shi (2015) A 2-D dysprosium-organic complex constructed from 6,7-dihydropyrido(2,3-d)pyridazine-5,8-dione and oxalic acid: synthesis, characterization and photoluminescence, Journal of Coordination Chemistry, 68:10, 1788-1799, DOI: 10.1080/00958972.2015.1023194

To link to this article: http://dx.doi.org/10.1080/00958972.2015.1023194

Accepted author version posted online: 26 Feb 2015.
Published online: 27 Mar 2015.

Journal of Coordination Chemistry, 2015
Vol. 68, No. 10, 1788–1799, http://dx.doi.org/10.1080/00958972.2015.1023194

A 2-D dysprosium-organic complex constructed from 6,7-dihydropyrido(2,3-*d*)pyridazine-5,8-dione and oxalic acid: synthesis, characterization and photoluminescence

YUNSHAN ZHOU*, JUNMEI SUN, WAQAR AHMAD, LIJUAN ZHANG* and ZONGHAI SHI

State Key Laboratory of Chemical Resource Engineering, Institute of Science, Beijing University of Chemical Technology, Beijing, PR China

(*Received 11 June 2014; accepted 18 February 2015*)

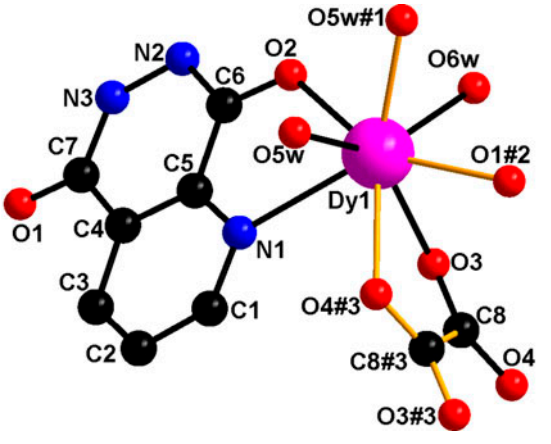

A pyridine derivative 6,7-dihydropyrido(2,3-*d*)pyridazine-5,8-dione (H_2PDH) and oxalic acid (H_2ox) are reacted with dysprosium oxide to develop a new 2-D dysprosium–organic complex [Dy(PDH)$(ox)_{0.5}(H_2O)_2$]. The single-crystal structure reveals that acylamino oxygens and coordinated waters develop a 3-D supramolecular network, which is composed of 2-D layers, and each 2-D layer is formed by 1-D Dy–H_2O–ox chains linked by tridentate PDH^{2-} ligands. The complex exhibits metal-centered luminescence with yellowish blue emission. The energy transfer mechanism and photoluminescence are also investigated.

Keywords: Dysprosium; Lanthanide–organic complex; Crystal structure; Energy transfer; Photoluminescence

*Corresponding authors. Email: zhouys@mail.buct.edu.cn (Y. Zhou); ljzhang@mail.buct.edu.cn (L. Zhang)

1. Introduction

Lanthanide–organic networks receive interest for fascinating architecture, excellent stability, and application as organic light-emitting diodes [1]. The popularity of lanthanide–organic coordination polymers for making highly electroluminescent devices owes to their inherent sharp emission bands and elevated internal quantum efficiency, which permit them as promising candidates for next generation of photoluminescent devices. The high photoluminescent intensity of Ln^{3+} 4f–4f transitions after harvesting of both singlet and triplet excitations by an appropriate "antenna" organic chromophore is an additional advantage of lanthanide complexes [2]. The most accepted mechanism of energy transfer from ligands to a lanthanide cation, as explained by Crosby and Whan [3], involves light absorption by organic chromophore to produce excited singlet states, intersystem crossing to populate the ligand triplet states, and energy transfer from the triplet states to the lanthanide emissive levels for light emission. Due to the key role of organic ligand in lanthanide–organic coordination polymers, there should be much attention in the structural choice of ligand. If the ligand has heteroatoms, such as N and O, aromaticity, isomerism, rigidity, and conjugation, it will surely be an excellent candidate for the sensitization of Ln^{3+} cations because the luminescent properties of lanthanide–organic coordination polymers mainly depend on the nature of chromophores [4].

Pyridine derivatives as antenna sensitizers have been used to construct lanthanide–organic coordination polymers because of their high aromatic character and coordination sites from the electron lone pair on nitrogen [5, 6]. Among the pyridine derivatives, 6,7-dihydropyrido(2,3-*d*)pyridazine-5,8-dione (H_2PDH) is rigid and has conjugation with different heteroatoms (N– and O–). This ligand (H_2PDH) was first used by our group to construct a series of mononuclear lanthanide complexes $[Ln(HPDH)_3(H_2O)_3]\cdot H_2O$ (Ln = Sm^{3+}, Eu^{3+}, Tb^{3+}, and Dy^{3+}) [7] and a series of 2-D lanthanide–organic complexes $[Ln(HPDH)(ox)(H_2O)]_n$ (Ln = Eu^{3+}, Tb^{3+}, Sm^{3+}, Gd^{3+}, ox = oxalate) [8]. Some factors such as temperature, pH, the molar ratio of the starting materials, the metal cations, etc. influence the results leading to different structures of the lanthanide–organic coordination polymers. For example, under the same experimental conditions, Eu^{3+}, Tb^{3+}, Sm^{3+}, Gd^{3+}, and Dy^{3+} reacted with H_2PDH and H_2ox to give two types of LnOFs, $[Ln(HPDH)(ox)(H_2O)]_n$ (Ln = Eu^{3+}, Tb^{3+}, Sm^{3+}, Gd^{3+}, ox = oxalate) [8] and $[Dy(PDH)(ox)_{0.5}(H_2O)_2]$ which are prepared in this work. Here, we report the synthesis, structure, and luminescence of a new $[Dy(PDH)(ox)_{0.5}(H_2O)_2]$ complex. The energy transfer mechanism of the complex was also studied.

2. Experimental

2.1. *Materials and methods*

All chemicals are of reagent grade quality, obtained from commercial sources, and used without purification. H_2PDH was synthesized according to the reported method [8]. IR (KBr pellets) spectra were recorded on a Nicolet® FT IR-170SX spectrometer from 4000 to 400 cm^{-1}. UV–vis spectra were recorded on a Shimadzu® UV-2550 spectrophotometer from 200 to 800 nm. Elemental analyses for C, H, and N were performed on a Perkin-Elmer® 240C analytical instrument, while analysis for Dy was performed using an ICPS-7500 model inductively coupled plasma emission spectrometer by dissolving the sample in dilute hydrochloric acid. Thermogravimetric analyses (TGA) and differential

thermal analysis (DTA) were performed on a NETZSCH STA 449C® unit at a heating rate of 10 °C min^{-1} under nitrogen. Powder X-ray diffraction (XRD) measurements were performed on a Rigaku-Dmax® 2500 diffractometer at a scanning rate of 15°/min in the 2θ range from 5° to 90° with graphite monochromated Cu Kα radiation (λ = 0.15405 nm). The photoluminescence spectra were recorded using a Hitachi® F-7000 FL spectrofluorimeter with both excitation and emission slits of 5 nm using a xenon arc lamp as the light source (150w), the photomultiplier tube voltage was 700 V, and the scan speed was 1200 nm min^{-1}.

2.2. *Synthesis of [Dy(PDH)(ox)$_{0.5}$(H$_2$O)$_2$]*

A mixture of H_2PDH (0.5 mM, 0.081 g), H_2ox (0.25 mM, 0.022 g), and Dy_2O_3 (0.12 mM, 0.046 g) was added to H_2O (10 mL), and then the mixture was poured in a Parr Teflon-lined stainless steel vessel (25 mL), heated to 170 °C for 96 h, and then cooled slowly to room temperature. Yellow needle crystals of [Dy(PDH)$(ox)_{0.5}(H_2O)_2$] were collected by filtration, washed with water, and C_2H_5OH correspondingly, and then dried in air. Yield: 0.0167 g (36.3% based on Dy). Anal. Calcd for $C_8H_7N_3O_6Dy$ (%): C, 23.80; H, 1.74; N, 10.41. Found: C, 23.57; H, 1.66; N, 10.04. FTIR (KBr, cm^{-1}): 1639(s), 1579(s), 1480(w), 1385(s), 1223(s), 1116(m), 808(s), 636(w), 515(m).

2.3. *X-ray crystallography*

Single-crystal XRD data of [Dy(PDH)$(ox)_{0.5}(H_2O)_2$] were collected on an Oxford Diffraction Xcalibur Eos Gemini diffractometer with Mo Kα radiation (λ = 0.71073 Å) in the ω scan mode. The structures were solved by direct methods and refined anisotropically using full-matrix least squares with the SHELX 97 program package [9]. The non-hydrogen

Table 1. Summary of crystallographic data for Dy(PDH)$(ox)_{0.5}(H_2O)_2$.

Formula	$C_8H_7DyN_3O_6$
*F*w	403.67
Crystal system	Triclinic
Space group	*P*-1
a (Å)	6.2367(4)
b (Å)	9.1911(7)
c (Å)	9.2901(5)
α (°)	86.515(5)
β (°)	71.798(5)
γ (°)	86.764(5)
V (Å^3)	504.56(6)
Z	2
ρ_{calcd} (mg m^{-3})	2.657
Temp (K)	101.6
F (0 0 0)	380.0
μ (mm^{-1})	7.432
Reflections collected/unique	3252
R(int)	0.0371
R_1, wR_2 [$I > 2\sigma(I)$]	0.0270, 0.0621
R_1, wR_2 (all data)	0.0288, 0.0631
GOF	1.063
Largest diff. peak and hole (e Å^{-3})	1.34 and −1.36

Table 2. Selected bond lengths (Å) and angles (°) in $Dy(PDH)(ox)_{0.5}(H_2O)_2$.

Bond lengths			
Dy1–O1#2	2.390(3)	Dy1–O5w	2.235(3)
Dy1–O2	2.371(4)	Dy1–O5w#1	2.268(4)
Dy1–O3	2.371(4)	Dy1–O6w	2.425(3)
Dy1–O4#3	2.474(2)	Dy1–N1	2.619(4)
Bond angles			
O(1)#2–Dy(1–O(2)	153.16(13)	O(2)–Dy(1)–O(4)#3	137.97(12)
O5w–Dy(1)–N(1)	80.68(13)	O(2)–Dy(1)–O(3)	103.08(13)
O5w–Dy(1)–O(4)#3	76.12(12)	O6w–Dy(1)–O(2)	73.61(12)
O(1)#2–Dy(1)–O(4)#3	68.17(11)	O5w#1–Dy(1)–O(2)	81.09(12)
O5w–Dy(1)–O(1)#2	97.77(12)	O(3)–Dy(1)–O6w	72.66(14)
O5w#1–Dy(1)–O(1)#2	81.66(12)	O5w#1–Dy(1)–O(3)	145.10(12)
O(3)–Dy(1)–O(1)#2	80.17(12)	O(3)–Dy(1)–O(4)#3	67.09(12)
O6w–Dy(1)–O(1)#2	82.26(12)	O(3)–Dy(1)–N(1)	77.118(14)
O(1)#2–Dy(1)–N(1)	140.16(14)	O(3)–Dy(1)–O5w	141.17(13)
O(2)–Dy(1)–N(1)	65.05(13)		

#1 = $-x+1, -y+1, -z+1$; #2 = $x, y, z+1$; #3 = $-x+1, -y+2, -z+1$; #4 = $x, y, z-1$.

atoms were located in successive difference Fourier syntheses; all hydrogens were placed in their geometric positions and refined isotropically. The final refinement was performed by full-matrix least-squares methods with anisotropic thermal parameters for non-hydrogen atoms on F^2 [10]. A summary of the crystallographic data and structural determination parameters are given in table 1. Selected bond lengths and angles are listed in table 2.

3. Results and discussion

3.1. *Structural description of $[Dy(PDH)(ox)_{0.5}(H_2O)_2]$*

Single-crystal X-ray analysis revealed that $[Dy(PDH)(ox)_{0.5}(H_2O)_2]$ possesses a 2-D layer network, which further constitutes a 3-D supramolecular structure. It crystallizes in space

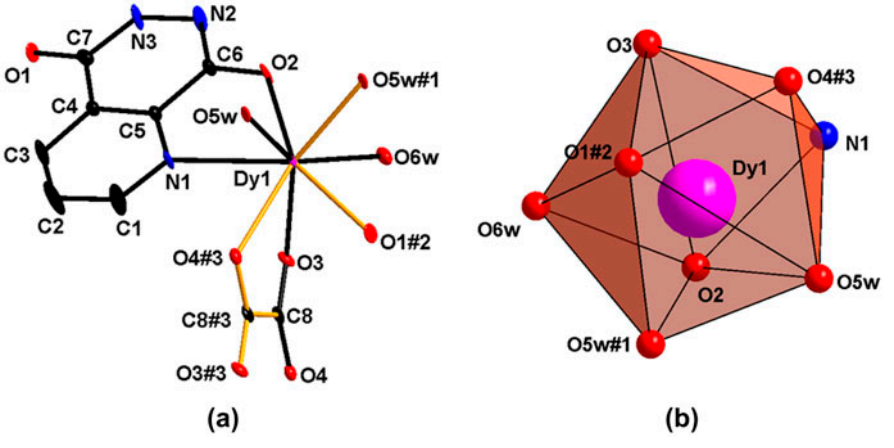

Figure 1. Perspective view of the local coordination environment of Eu^{3+} in $Dy(PDH)(ox)_{0.5}(H_2O)_2$ with thermal ellipsoids drawn at 50% probability showing the labeling scheme (all hydrogens are omitted for clarity) (a) and coordination polyhedron of $Dy(PDH)(ox)_{0.5}(H_2O)_2$ (b). Symmetry codes: #1 $-x+1, -y+1, -z+1$; #2 $x, y, z+1$; #3 $-x+1, -y+2, -z+1$; #4 $x, y, z-1$.

group *P*-1, and the asymmetric unit is composed of one Dy^{3+}, one PDH^{2-} ligand, half of one oxalate (ox^{2-}), and two coordinated waters (O5w and O6w) [figure 1(a)]. The coordination polyhedron around Dy^{3+} can be described as a distorted dodecahedral geometrical shape with a coordination number of eight [figure 1(b)]. As shown in figure 1(a), the eight-coordinate Dy^{3+} is coordinated by two acylamino oxygens (O1#2 and O2) of two different PDH^{2-} ligands, one pyridyl nitrogen (N1) of one PDH^{2-} molecule, two oxygens (O3 and O4#3) from one ox^{2-}, and three oxygens (O5w, O5w#1, and O6w) from three coordinated waters.

The seven Dy–O bond lengths of the complex vary from 2.235(3) to 2.474(2) Å and Dy1–$N_{pyridyl}$ (N1) bond length is 2.619(4) Å (table 2). For comparison, it should pointed out that Eu–O distances are 2.363(24)–2.457(23) Å and Eu–N distance is 2.604(31) Å in $[Eu(HPDH)_3(H_2O)_3]\cdot H_2O$ [7], Sm–O distances are 2.3519(2)–2.5680(3) Å and Sm–N distance is 2.6340(3)–2.7412(5) Å in $Sm(HPDH)(ox)(H_2O)]_n$ [8]. The results indicate that Ln–O and Ln–N distances increase basically with the increase of Ln^{3+} ion radius.

Each PDH^{2-} adopts a biconnected μ^2-(η^1, η^1, η^1) tridentate coordination mode, the pyridyl N and acylamino O chelate one Dy^{3+} center, while another acylamino O atom coordinates with second Dy^{3+} center. Oxalate links two Dy^{3+} centers and adopts a biconnected tetradentate μ^2-(η^1, η^1, η^1, η^1) coordination mode (scheme 1) [11].

The structure of the complex can be depicted as follows: first, a pair of waters (O5w and O5w#3) bridge a pair of Dy^{3+} centers resulting in a $[Dy_2(H_2O)_2]^{6+}$ dimer (Dy_2O_2 core); within the dimer, the Dy···Dy distance is 3.6702(4) Å, which is shorter than 4.5826(6) Å of the La···La distance in $[La_2(H_2O)_2]^{6+}$ dimer [12] owing to the longer radius of La^{3+}. The adjacent $[Dy_2(H_2O)_2]^{6+}$ dimer and ox^{2-} ligand link each other alternately forming a 1-D

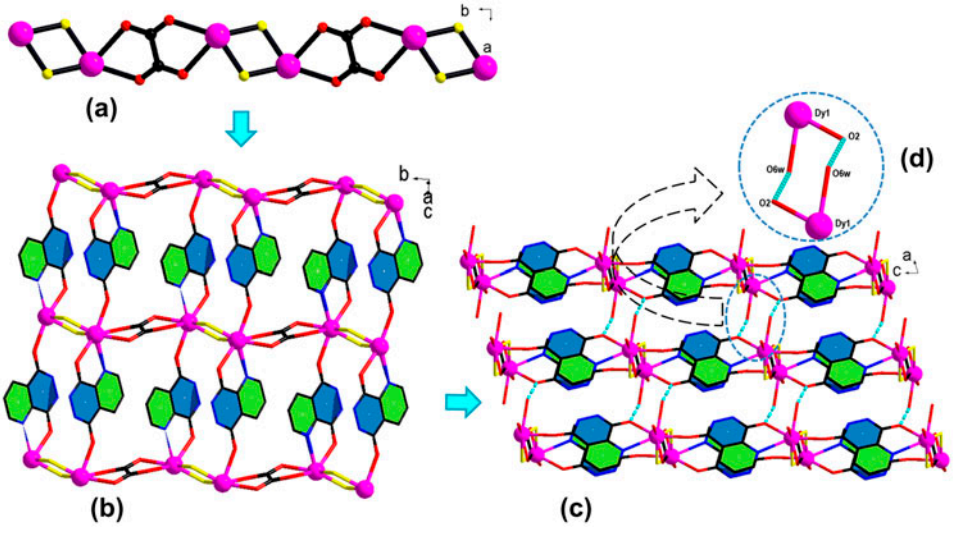

Figure 2. The schematic representation for the formation of 3-D supramolecular network: (a) A single 1-D infinite chain (–Dy–H_2O–Dy–ox–) of the complex along the *b* direction; the water molecules in the chain are represented by yellow colored balls; (b) The formation of a 2-D layer from infinite 1-D chains; the blue ring shows pyridazine ring, while green shows pyridine ring and also the water molecules in 1-D chains are represented by yellow color; (c) Formation of 3-D supramolecular network through hydrogen bonds between neighboring 2-D layers; (d) The enhanced sketch of hydrogen bonds (broken lines) between O2 and O6w. The coordinated water molecules (O6w) are omitted for clarity in (a) and (b). Color code: Dy, purple; O, red; C, black (see http://dx.doi.org/10.1080/00958972.2015.1023194 for color version).

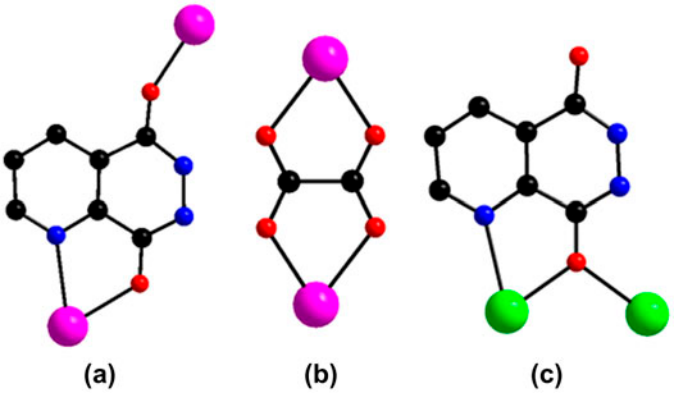

Scheme 1.

Dy–H_2O-ox chain along the *b* direction. The Dy···Dy distance bridged by oxalate is 6.1880 (6) Å [figure 2(a)], which lies in the range of reported Dy complexes (6.173–6.40 Å) bridged by oxalate [13]. The adjacent 1-D chains then link each other through PDH^{2-} ligands to form a 2-D layer network in the *bc* plane [figure 2(b)]. The distance of the adjacent 1-D chains in the 2-D layer along the *c* axis is 9.2901(6) Å based on the shortest distance of Dy···Dy. Extensive hydrogen bonds exist besides the covalent bonding within the 2-D layer, viz., O6w···O5w = 2.8772 Å, O5w···O2 = 3.0160 Å, O6w···O3 = 2.8421 Å, and O5w···O4 = 2.9096 Å.

In a 2-D layer, each PDH^{2-} ligand bridges two Dy(III) centers, while these Dy^{3+} centers are bridged through pairs of waters and oxalates alternatively to form two kinds of macropores (A and B) (figure 3). Each macropore of A is an 18-membered $Dy_4(PDH)_2(H_2O)_2$

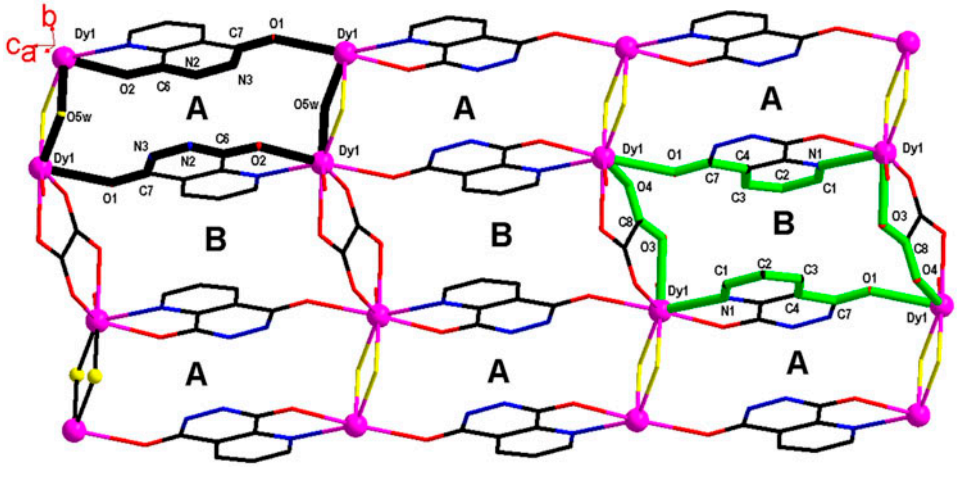

Figure 3. The 2-D layer structure containing two different macrocycles (A: Black 18-membered $Dy_4(PDH)_2(H_2O)_2$ macrocycle; B: Green 24-membered $Dy_4(PDH)_2(ox)_2$ macrocycle). Color code: Dy, purple; O, red; C, black; N, blue. The water molecules in 1-D chains are represented by yellow color (see http://dx.doi.org/10.1080/00958972.2015.1023194 for color version).

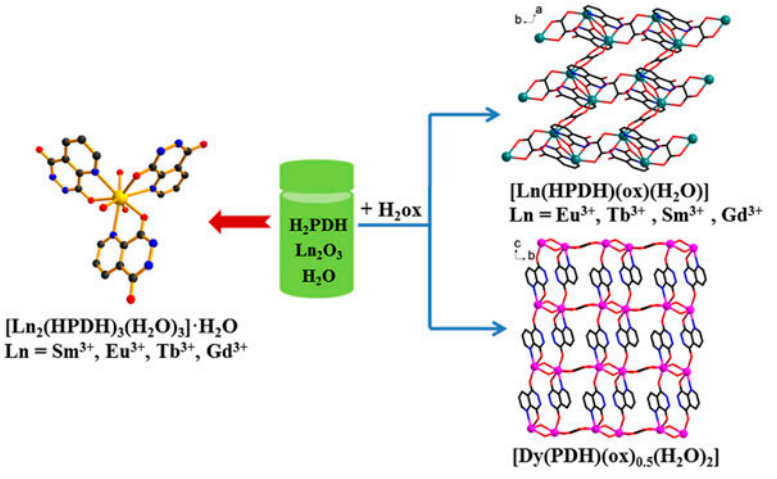

Scheme 2.

structure with size *ca*. 9.29 Å × 3.67 Å based on Dy···Dy distances and the second macropore of B is 24-membered $Dy_4(PDH)_2(ox)_2$ with size *ca*. 9.29 Å × 6.19 Å based on Dy···Dy distances.

Further scrutiny of the framework reveals two types of intralayered $\pi\cdots\pi$ stacking interactions: the first is $\pi\cdots\pi$ stacking interaction with the centroid–centroid distance of 3.5156 Å between adjacent pyridazine rings (N2, N3, C4, C5, C6, and C7) and (N2, N3, C4, C5, C6, and C7) and the second with the centroid–centroid distance of 3.6183 Å is between (N1, C1, C2, C3, C4, and C5) and (N1, C1, C2, C3, C4, and C5) pyridine rings of adjacent H_2PDH ligands (figure 4). The interlayered hydrogen bonds between O6w and O2 atoms (O6w···O2 = 2.8718 Å) from two adjacent 2-D layers [figure 2(c) and (d)] lead to the formation of 3-D supramolecular network of complex [figure 2(c)].

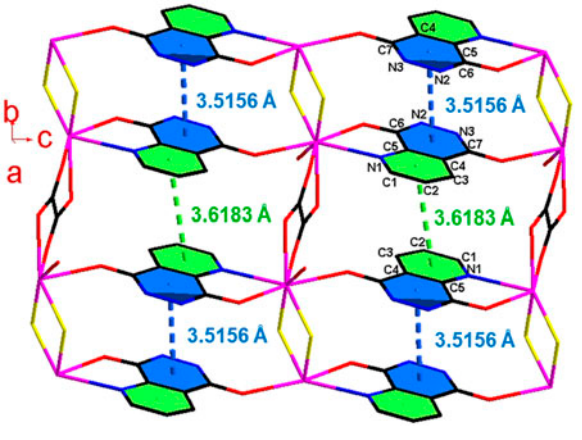

Figure 4. Short-range interactions ($\pi - \pi$) within a 2-D layer in $Dy(PDH)(ox)_{0.5}(H_2O)_2$. Color code: Dy, purple; O, red; C, black; N, blue. The water molecules in 1-D chains are represented by yellow color (see http://dx.doi.org/10.1080/00958972.2015.1023194 for color version).

Notably, the reaction between Ln_2O_3, H_2PDH, and H_2ox under the same conditions generated two kinds of structures [Ln(HPDH)(ox)(H_2O)] (Ln = Eu^{3+}, Tb^{3+}, Sm^{3+}, and Gd^{3+}) [8] and [Dy(PDH)$(ox)_{0.5}(H_2O)_2$] in this work. The main differences between the two types of structures are as follows: the coordination modes of H_2PDH are different in the two types of complexes. In [Ln(HPDH)(ox)(H_2O)], each $HPDH^-$ ligand is a biconnected μ^2-(η^1, η^2) tridentate coordination where its pyridyl N and acylamino O coordinate to two Ln(III) centers, while in [Dy(PDH)$(ox)_{0.5}(H_2O)_2$], each PDH^{2-} ligand adopts a biconnected μ^2-(η^1, η^1, η^1) tridentate coordination mode, the pyridyl N and acylamino O chelate one Dy^{3+} center, while another acylamino O coordinates with second Dy^{3+} center. In [Ln(HPDH)(ox)(H_2O)], Ln^{3+} and ox^{2-} connect each other alternately to form a 1-D Ln-ox chain, then the neighboring 1-D chains interconnect by $HPDH^-$ ligands to form a 2-D network in the *ab* plane (scheme 1). While in [Dy(PDH)$(ox)_{0.5}(H_2O)_2$], the 1-D Dy–H_2O–ox chain is formed through the alternate connection of $[Dy_2(H_2O)_2]^{6+}$ and ox^{2-}, and then the adjacent 1-D chains link each other through PDH^{2-} ligands to form a 2-D layer network in the *bc* plane.

Based on our present and previous investigation [7, 8], H_2PDH reacted with Ln_2O_3 (Ln = Sm, Eu, Tb, and Dy) leading to a series of mononuclear complexes [Ln(HPDH)$(H_2O)_3$]·H_2O [7], while the reaction of H_2PDH and Ln_2O_3 in the presence of H_2ox generated two kinds of complexes with 2-D layer structures, $[Ln(HPDH)(ox)(H_2O)]_n$ (Ln = Eu^{3+}, Tb^{3+}, Sm^{3+}, Gd^{3+}, and Dy^{3+}) [8] and [Dy(PDH)$(ox)_{0.5}(H_2O)_2$] (scheme 2). The presence of H_2ox resulted in the formation of 2-D layer structures due to its bridging function, while the diversities of the resulting structures with respect to different Ln^{3+} cations prepared under the same reaction condition may be tentatively explained as follows: The radii decrease in the order $Sm^{3+} > Eu^{3+} > Gd^{3+} > Tb^{3+} > Dy^{3+}$, the oxalate is rigid due to the sp^3 hybridization adopted by C. Unlike the situation for bigger Ln^{3+}, the smallest Dy^{3+} prefers to take two bridging water molecules (the bond angle of Ow5–Dy1–Ow5 is 70.88°) rather than oxalate [the bond angle of O3(from oxalate)–Dy1–O4(from oxalate) is 67.07°] in order to minimize the repulsion between the coordinating atoms and consequently minimize the energy of the system, although the difference among their radii is not very big due to lanthanide contraction.

3.2. *Powder XRD*

The experimental PXRD patterns of [Dy(PDH)$(ox)_{0.5}(H_2O)_2$] match with its simulated ones, indicating the phase purity of the bulk materials. The variation in reflection intensities among the simulated and experimental patterns is due to the superior orientation of the powder sample during collection of the experimental PXRD data (figure 5).

3.3. *Thermal analysis*

To study the thermal stability of the complex, TGA–DTA were performed (figure 6). Two-step weight loss from 20 to 800 °C can be observed in the TGA–DTA curve. The first step of weight loss at 20 to 149.8 °C can be attributed to loss of two coordinated waters and half of CO_2 (weight loss calcd: 10.25%, found: 9.65%), then from 174.3 to 276.3 °C, the complex started the second step of weight loss of 43.47% (calcd: 43.65%) corresponding to loss of all organic moieties (figure 6). The weight of the remaining residue (calcd 46.20%, found

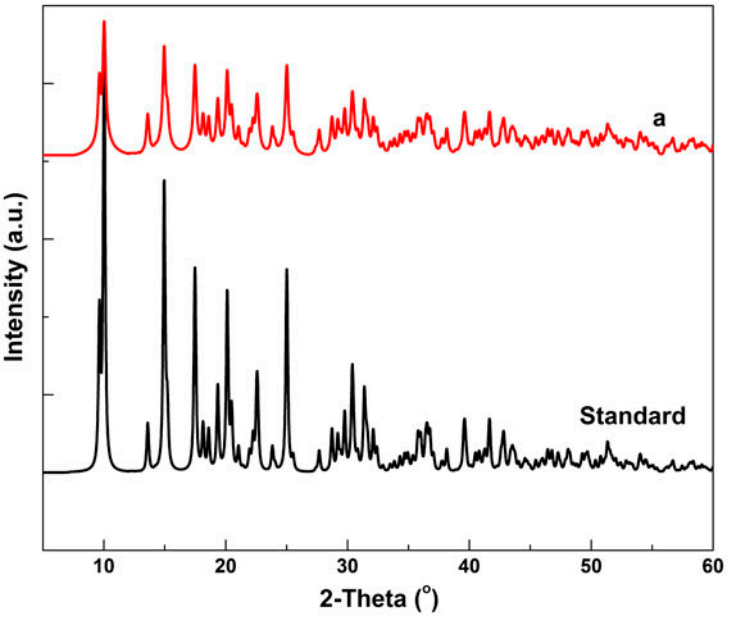

Figure 5. XRD analysis pattern of simulated and experimental (line a) of $Dy(PDH)(ox)_{0.5}(H_2O)_2$.

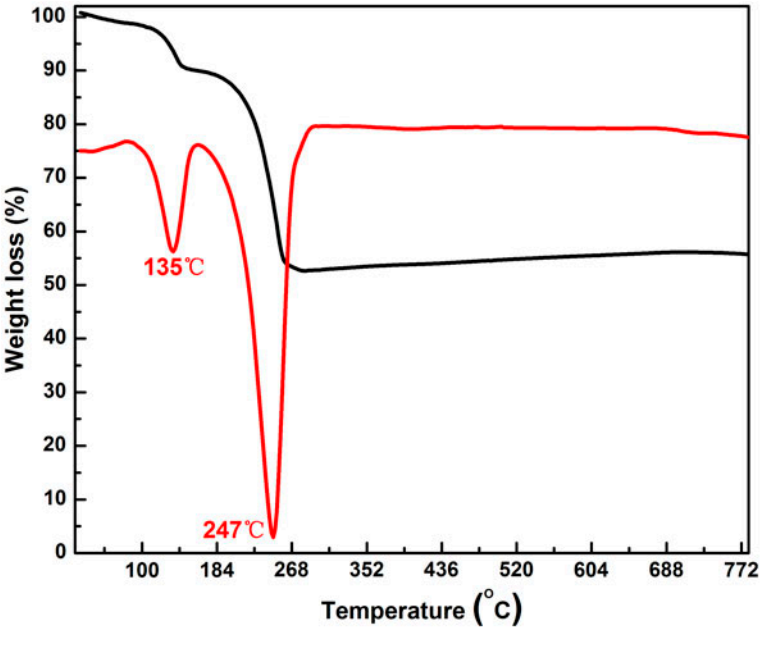

Figure 6. TGA and DTA curves of $Dy(PDH)(ox)_{0.5}(H_2O)_2$.

46.88%) matches nicely the composition of Dy_2O_3. The endothermic DTA curves at 135 and 247 °C can be observed along with the weight loss process.

3.4. *Photoluminescence properties*

To understand the energy transfer processes of the complex, the singlet and the triplet energy levels ($^3\pi\pi^*$) of H_2PDH which were determined in our published work [8] and H_2ox ligands [14] were compared with excited resonance energy level ($^4F_{9/2}$) of Dy^{3+}. The energy gap $\Delta E(^1\pi\pi^*–^3\pi\pi^*)$ of 12,936 cm^{-1} for H_2PDH [8] indicated that the intersystem crossing process is effective in the complex (figure 7) [15]. The energy gaps $\Delta E(^3\pi\pi^* - {}^4F_{9/2})$ of H_2PDH ($^3\pi\pi^* = 21$, 786 cm^{-1}) and H_2ox ($^3\pi\pi^* = 23$, 753 cm^{-1}) [8] and the excited resonance energy level ($^4F_{9/2}$) of Dy^{3+} (21,000 cm^{-1}) were 786 cm^{-1} and 2753 cm^{-1}, respectively. The energy gaps between the triplet level ($^3\pi\pi^*$) of ligand (H_2PDH/H_2ox) and resonating energy level ($^4F_{9/2}$) of Dy^{3+} imply that H_2ox is more suitable sensitizer for Dy^{3+} as compared to H_2PDH in this study [16].

The excitation spectrum of the complex under emission of 481 nm exhibit three main peaks at 218, 255, and 270 nm and some characteristic features corresponding to the metal-centered transition at 364 nm ($^4M_{9/2} \leftarrow {}^6H_{15/2}$), 388 nm ($^4F_{7/2} \leftarrow {}^6H_{15/2}$) and 433 nm ($^4G_{11/2} \leftarrow {}^6H_{15/2}$) for the Dy(III) complexes [7]. The emission spectrum shows two apparent emission bands at 481 nm ($^4F_{9/2} \rightarrow {}^6H_{15/2}$) and 573 nm ($^4F_{9/2} \rightarrow {}^6H_{13/2}$) under excitation of 255 nm (the strongest bands in the excitation spectrum) (figure 8) [17]. This complex exhibits typical yellowish blue emission of Dy^{3+} for $^4F_{9/2} \rightarrow {}^6H_n$ (n = 15/2, 13/2) transitions as

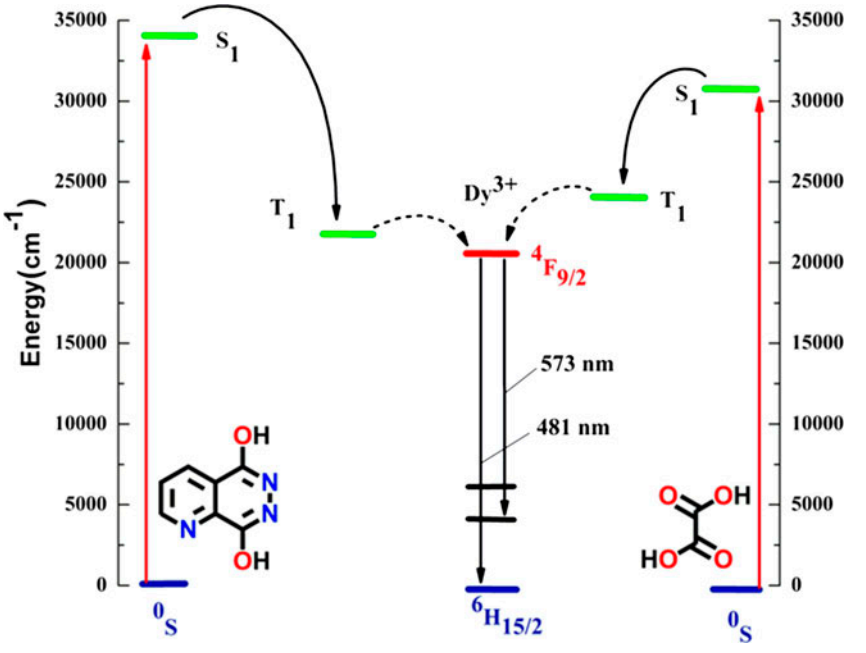

Figure 7. Partial energy diagrams for Dy^{3+}. The main luminescent level is drawn in red, while the fundamental levels are indicated in blue; singlet and triplet energy levels of H_2PDH and H_2ox ligands in green (see http://dx.doi.org/10.1080/00958972.2015.1023194 for color version).

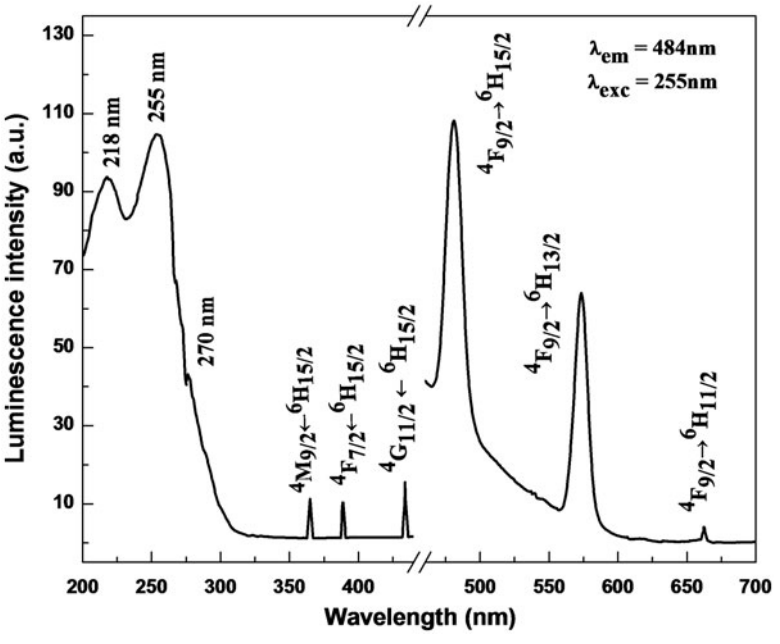

Figure 8. Excitation and emission spectra of $Dy(PDH)(ox)_{0.5}(H_2O)_2$ at $\lambda_{em} = 484$ nm and $\lambda_{exc} = 255$ nm, respectively.

the intensity of the blue emission, corresponding to the $^4F_{9/2} \rightarrow {}^6H_{15/2}$ transition, is a little stronger than that of the yellow one $^4F_{9/2} \rightarrow {}^6H_{13/2}$ [18]. A weak band centered at 663 nm may be attributed to the $^4F_{9/2} \rightarrow {}^6H_{11/2}$ transition (figure 8) [14].

4. Conclusion

A new 2-D dysprosium–organic network has been hydrothermally synthesized using H_2PDH and oxalic acid ligands. The complex is composed of 2-D layers which are formed by 1-D Dy–H_2O–ox chains linked by PDH^{2-} ligands. The luminescent properties and energy transfer mechanism of the complex were investigated, indicating that oxalic acid acts as better sensitizer toward Dy^{3+} than H_2PDH, and the complex exhibits typical yellowish blue emission. Considering the fact that H_2PDH possesses rich coordination chemistry due to its rigidity and conjugation with different heteroatoms (N– and O–), a variety of complexes of new structures and interesting properties are expected by reacting H_2PDH in the presence/absence of other proper secondary ligands with deliberately selected metal cations such as transition metal, lanthanide, and actinide cations having different radii and electronic structures; relevant work is underway in our lab.

Supplementary material

CIF file for the structure reported in this article has been deposited with the Cambridge Crystallographic Data Center (CCDC No. 960627).

Acknowledgements

The financial support of the NSFC, PCSIRT (No. IRT1205), and the fundamental research funds for the central universities (YS1406) is greatly acknowledged. Prof. Xue Duan of Beijing University of Chemical Technology is greatly acknowledged for his kind support.

Disclosure statement

No potential conflict of interest was reported by the authors.

Supplemental data

Supplemental data for this article can be accessed here [http://dx.doi.org/10.1016/j.inoche.2013.11.033].

References

[1] (a) I. Hemmilä, V. Laitala. *J. Fluoresc.*, **15**, 529 (2005); (b) S. Tanabe. *C. R. Chim.*, **5**, 815 (2002); (c) J.-C.G. Bunzli, C. Piquet. *Chem. Soc. Rev.*, **34**, 1048 (2005); (d) F. Marchetti, C. Pettinari, R. Pettinari. *Coord. Chem. Rev.*, **249**, 2909 (2005).
[2] (a) J. Kido, K. Nagai, Y. Ohashi. *Chem. Lett.*, **19**, 657 (1990); (b) J. Kido, K. Nagai, Y. Okamoto. *J. Alloys Compd.*, **192**, 30 (1993); (c) T. Sano, M. Fujita, T. Fujii, Y. Hamada, K. Shibata, K. Kuroki. *Jpn. J. Appl. Phys.*, **34**, 1883 (1995).
[3] (a) R.E. Whan, G.A. Crosby. *J. Mol. Spectrosc.*, **8**, 315 (1962); (b) G.A. Crosby, R.E. Whan, R.M. Alire. *J. Chem. Phys.*, **34**, 743 (1961); (c) G.A. Crosby, R.E. Whan, J.J. Freeman. *J. Phys. Chem.*, **66**, 2493 (1962).
[4] C.A. Bauer, T.V. Timofeeva, T.B. Settersten, B.D. Patterson, V.H. Liu, B.A. Simmons, M.D. Allendorf. *J. Am. Chem. Soc.*, **129**, 7136 (2007).
[5] (a) Y.K. Park, S.B. Choi, H. Kim, K. Kim, B. Won, K. Choi, J. Choi, W. Ahn, N. Won, S. Kim, D.H. Jung, S. Choi, G. Kim, S. Cha, Y.H. Jhon, J.K. Yang, J. Kim. *Angew. Chem. Int. Ed.*, **46**, 8230 (2007); (b) M. Zhang, J. Zhang, S. Zheng, G. Yang. *Angew. Chem. Int. Ed.*, **44**, 1385 (2005).
[6] J. Jin, F. Bai, G. Li, M. Jia, J. Zhao, H. Jia, J. Yu, J. Xu. *CrystEngComm.*, **14**, 8162 (2012).
[7] W. Ahmad, L. Zhang, Y. Zhou. *Photochem. Photobiol. Sci.*, **13**, 660 (2014).
[8] W. Ahmad, L. Zhang, Y. Zhou. *CrystEngComm.*, **16**, 3521 (2014).
[9] (a) G.M. Sheldrick, *SHELXTL V5.1, Software Reference Manual*, Bruker AXS, Inc., Madison, WI (1997); (b) W.S. Sheldrick, M. Morr. *Acta Crystallogr., Sect. B*, **37**, 733 (1981).
[10] (a) G.M. Sheldrick, *SHELXTL-97, a Program for Crystal Structure Refinement*, University of Göttingen, Germany (1997); (b) G.M. Sheldrick. *SHELXS97, Program for Crystal Structure Solution*, University of Gottingen, Gottingen, Germany (1997).
[11] P.D. Knight, P. Scott. *Coord. Chem. Rev.*, **242**, 125 (2003).
[12] Y. Li, F.K. Zheng, X. Liu, W.Q. Zou, G.C. Guo, C.Z. Lu, J.S. Huang. *Inorg. Chem.*, **45**, 6308 (2006).
[13] (a) G.H. Du, X.Y. Kan, H.N. Li. *Polyhedron*, **30**, 3197 (2011); (b) J. Xu, J.W. Cheng, W.P. Su, M.C. Hong. *Cryst. Growth Des.*, **11**, 2294 (2011); (c) Y.J. Zhang, M. Bhadbhade, N. Scales, I. Karatchevtseva, J.R. Price, K. Lu, G.R. Lumpkin. *J. Solid State Chem.*, **219**, 1 (2014).
[14] P. Wang, R. Fan, X. Liu, L. Wang, Y. Yang, W. Cao, B. Yang, W. Hasi, Q. Su, Y. Mu. *CrystEngComm.*, **15**, 1931 (2013).
[15] (a) L. Armelao, S. Quici, F. Barigelletti, G. Accorsi, G. Bottaro, M. Cavazzini, E. Tondello. *Coord. Chem. Rev.*, **254**, 487 (2010); (b) W.T. Carnall, P.R. Fields, K. Rajnak. *J. Chem. Phys.*, **49**, 4443 (1968).
[16] M.V. Lucky, S. Sivakumar, M.L.P. Reddy, A.K. Paul, S. Natarajan. *Cryst. Growth Des.*, **11**, 857 (2011).
[17] X. Han, J. Lin, Z. Li, X. Qi, M. Li, X. Wang. *J. Rare Earths*, **26**, 904 (2008).
[18] (a) W.T. Wu, S.Y. He, H.M. Hu, M.L. Yang, Y.Y. Wang, Q.Z. Shi. *J. Coord. Chem.*, **60**, 1785 (2007); (b) J. Wang, Q. Han, J. Niu. *J. Coord. Chem.*, **57**, 33 (2004).